

Engineering correlated disorder for exotic light scattering diagrams

Denis Langevin,^{1,*} Emma Bosbaty-Galliot,² Emmanuel Centeno,² Pauline Bennet,¹
Rémi Carminati,^{3,4} Bodo D. Wilts,⁵ Patrick Bouchon,⁶ and Antoine Moreau²

¹*Aix Marseille Univ, CNRS, Université de Toulon, IM2NP, UMR 7334, F-13397 Marseille, France*

²*Université Clermont Auvergne, CNRS, Institut Pascal, F-63000 Clermont-Ferrand, France*

³*Institut Langevin, ESPCI Paris, Université PSL, CNRS, F-75005 Paris, France*

⁴*Institut d'Optique Graduate School, Université Paris-Saclay, Palaiseau, France*

⁵*Department of Chemistry and Physics of Materials,
University of Salzburg, AT-5020 Salzburg, Austria*

⁶*DOTA, ONERA, Université Paris-Saclay, Palaiseau, France*

(Dated: February 20, 2026)

Diffuse scattering of light from disordered assemblies is traditionally viewed as an uncontrollable broadband scattering background resulting in whitish hues. Here, we demonstrate that correlated disorder enables precise engineering of light scattering from 2D arrays of emitters resulting in strong observable colors. Our analytical framework shows that introducing controlled noise, with tunable probability density functions and correlations, generates three distinct scattering components: diffraction orders, diffuse background, and correlation halos. Correlation halos, often mistaken for broadened diffraction peaks, are independent features whose positions depend on correlation range and can appear between Bragg peaks. Crucially, they persist far beyond the regime where diffraction orders vanish. The noise probability density function provides an additional control: specific diffraction orders can be selectively suppressed while preserving others. This approach reproduces the scattering signatures of natural photonic structures, e.g. found in *Morpho* butterflies, and reveals multiple pathways from order to disorder, each with distinct optical properties. Our work provides a practical method for inverse design—finding the disorder that produces desired scattering patterns. This establishes diffuse scattering as a designable quantity, expanding the toolkit for metasurfaces and structural color beyond periodic and hyperuniform structures.

Natural photonic structures present a compelling paradox. Butterfly wing scales, bird feathers, and beetle cuticles often exhibit quasi-periodic arrangements of nanostructures that produce distinctive optical signatures – broad diffraction features centered on the positions of the Bragg peaks of the perfect crystals[1–6]. When one attempts to model these structures by adding noise to periodic lattices, the standard approach using white noise completely destroys the diffraction peaks, leaving only diffuse scattering [7–9]. This failure has sparked debates about whether the observed patterns truly arise from perturbed periodicity or require entirely different mechanisms. It has also made the optical properties of these natural structures difficult to reproduce with perfect accuracy [9–11].

The study of correlated disorder, and especially the discovery of hyperuniformity, marked a turning point in the understanding of disordered systems, demonstrating that correlations in disorder can lead to unexpected transparency and other remarkable properties[12–16]. This finding suggested that the transition from disorder to order could be controlled through correlation strength [17]. However, this perspective implicitly assumes only a single path: increasing correlations progressively transforms disorder into order. In reality, when studying quasi-periodic structures abundant in nature, the phase and property space of order and disorder appears far

richer [18–21]. Other studies have developed analytical frameworks to describe these phenomena [22, 23], but this work presents a more general formula providing the necessary understanding to design new structures.

Here, we advance our understanding of disordered systems by studying the multiple paths from perfect periodicity to complete disorder. We show that the correct tools to describe these structures are the probability density function and the correlation properties of the perturbative noise added to a periodic lattice. Through analytical treatment of far-field scattering, we identify three distinct components in reciprocal space: traditional diffraction orders, diffuse background, and a previously unrecognized term we call “correlation halos.” These halos, which appear often –but not exclusively– around Bragg peak positions, exhibit remarkable resilience: while diffraction orders decay rapidly with increasing disorder, correlation halos persist much further along the path toward randomness when correlations are properly tuned.

Our framework shows that the noise probability density function provides an additional powerful degree of freedom: individual diffraction orders that can be selectively suppressed or eliminated while preserving or enhancing others. Combined with correlation control, this enables a precise tailoring of scattering properties. We provide both the theoretical foundation and practical methods for generating these tailored noise distributions, establishing correlated disorder not as a perturbation that is to be minimized, but as a design tool for engineering light-matter interactions with capabilities ex-

* Contact author: denis.langevin@polytechnique.org

tending beyond those found in natural structures.

To understand how introducing disorder in a regular structure can produce such a diversity of responses, we first established a theoretical framework for one-dimensional quasi-periodic structures with controlled perturbations. We consider the positions x_n of nanostructures defined by:

$$x_n = n \times d + \epsilon_n, \quad (1)$$

where d is the average spacing (quasi-period) and ϵ_n a random variable representing the disorder.

We further define $\Delta_m^{(j)} = \epsilon_{j+m} - \epsilon_j$, a random variable derived from ϵ_n . $\Delta_m^{(j)}$ allows a characterization and/or control of the correlations between positions at distance $m d$. Controlling the ϵ and Δ random variables allows us to tune the scattering behavior of the structure, as will be shown below.

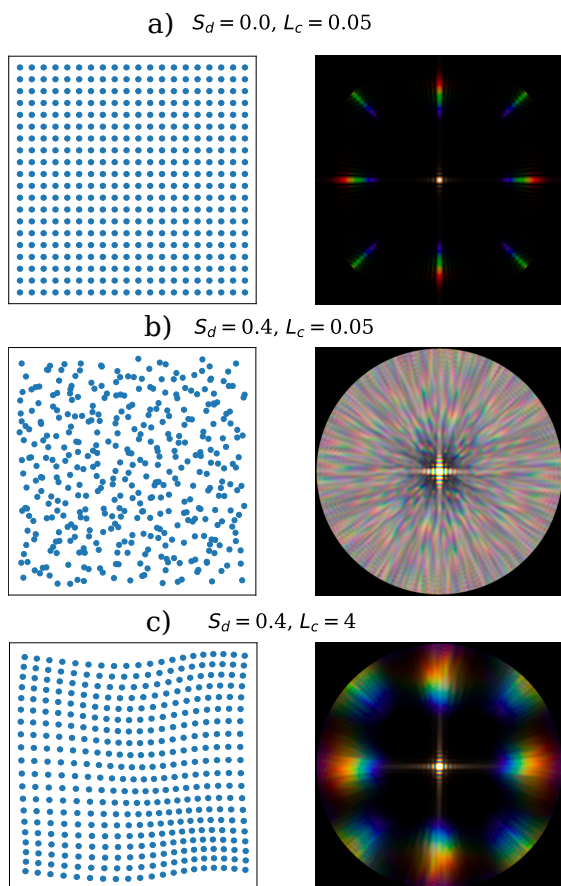


FIG. 1. (a–c) Angular distribution of the scattered light intensity from disordered geometries with different degrees of disorder. The left panels show examples of 20x20 quasi-periodic ensembles of points, for different values of S_d and L_c , generated using Eq. 2. The right panels show calculated k-space scattering patterns obtained from incident white light by a 20 x 20 ensemble of scatterers, averaged over 5 random ensembles. Note the difference in angular properties and color clarity.

To control the perturbations added to the underlying

periodic positions, we define i) the standard deviation of the added perturbations $S_d = \sqrt{\text{Var}(\epsilon)}$, which directly measures the intensity of the random noise, and ii) the correlation length L_c , which measures how far apart nanostructure positions are correlated. The exact definition of L_c depends on the type of noise used, but it typically varies between $L_c = 0$ (no correlations, *i.e.*, white noise) and a few periods (up to $5 \times d$). In the following, we will use $d = 1$, so that L_c and S_d are dimensionless quantities, and our results can be scaled to any spectral range.

These definitions can be extended to 2D (x, y) arrangements, by introducing independent $S_{d,x}$ and $S_{d,y}$ variables for the standard deviation of added perturbations, and $L_{c,x}$ and $L_{c,y}$ for the correlation length. Extension to arrangements where the height of each nanostructure is different and potentially correlated, *i.e.* thin (x, y, z) arrangements, is possible, but not discussed in this work.

Fig. 1 shows three examples of 2D quasi-periodic arrangements (with the positions of 20 x 20 nanostructures) with different values of $S_d = S_{d,x} = S_{d,y}$ and $L_c = L_{c,x} = L_{c,y}$ with their corresponding light scattering pattern. To generate these structures, we used Gaussian noise, with S_d and L_c controllable independently. To obtain N perturbations to the periodic positions (period d), we use Gaussian variables defined as ϵ_j :

$$\epsilon_j = S_d \frac{\text{Re} \left(\sum_{n=1}^{4\sigma} e^{i\phi_n} e^{-\frac{n^2}{2\sigma^2}} e^{2i\pi \frac{nj}{N}} \right)}{\sqrt{\sum_{n=1}^{4\sigma} e^{-\frac{n^2}{\sigma^2}}}}, \quad (2)$$

where ϕ_n are independent random phases, uniformly distributed in $[0, 2\pi]$, and $\sigma = \frac{N}{2\pi L_c}$. The denominator is a normalization term, equal to the standard deviation of the numerator.

With this equation, $\{\epsilon\}_j$ follows a Gaussian distribution with zero mean and variance S_d^2 . The $\{\Delta\}_m$ are also centered Gaussian variables, but with variance:

$$\text{Var}(\Delta_m) = 4S_d^2 \frac{\sum_{n=1}^{4\sigma} e^{-\frac{n^2}{\sigma^2}} \sin^2 \left(\pi \frac{nm}{N} \right)}{\sum_{n=1}^{4\sigma} e^{-\frac{n^2}{\sigma^2}}}. \quad (3)$$

In Fig. 1 the effect of S_d is straightforward: it controls how far from the periodic positions each nanostructure can be, and therefore how different the scattered intensity is from Bragg peaks.

Interpreting the effect of L_c , however, is more subtle: all we can observe is that it adds some regularity in the resulting positions and concentrates the scattered intensity around the diffraction peaks. This is due to the fact that L_c controls how many terms are involved in the summation in Eq. 2. For vanishing values of L_c , an infinite number of terms are taken into account, averaging their contributions such that $\text{Var}(\epsilon_{m+j} - \epsilon_j) = \text{Var}(\Delta_m) = 2S_d^2 = 2\text{Var}(\epsilon)$, corresponding to a case where the ϵ are uncorrelated, leading to a typical white noise pattern in reciprocal space (see Fig. 1 b). On the other hand, Fig. 1

c) shows that a structure with a high L_c will exhibit a very anisotropic scattered light diagram.

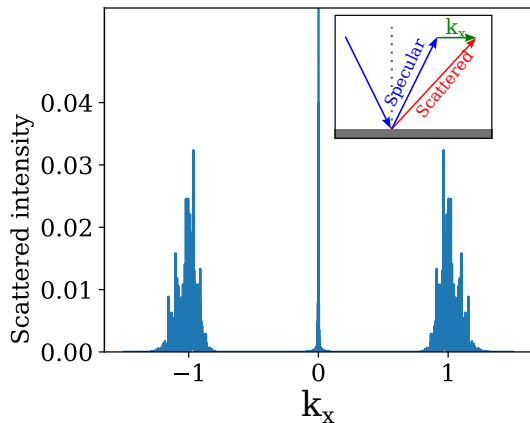


FIG. 2. Scattered intensity by a structure with 1000 nanostructures, $S_d = 0.45$, $L_c = 4.5$, no averaging. (inset): Definition of the k_x in-plane scattering wavevector

To better understand how a high L_c structure scatters light, we study 1D structures. Figure 2 shows the scattered intensity diagram, as a function of k_x , the normalized in-plane wavevector of light, for a 1D structure generated with the above disorder ($S_d = 0.45$, $L_c = 4.5$). We observe no diffraction peaks, but the smoothly varying lobes we have called correlation halos, here centered around the diffraction peak positions, as are often observed in naturally-occurring structures [5, 24, 25]. This demonstrates that this type of correlated disorder, when added as a perturbation to a periodic arrangement, can eliminate the diffraction peaks while preserving the correlation halos that we shall now investigate using a theoretical model.

The far-field scattered intensity of a quasi-periodic arrangement can be computed analytically, both to speed up the computations but also to better understand the underlying phenomena. To do so, we will make a few simplifying assumptions. First, we will assume that the nanostructures emit/reflect light isotropically, to distinguish the influence of the nanostructures from that of their positions (this amounts to neglecting the form factor of the structures and only modeling the structure factor). This is particularly relevant in our case because naturally-occurring structures tend to be composed of mostly locally identical nanostructures, *i.e.* the influence of their individual shape appear as a general prefactor to the scattered light intensity described in the following. Second, we will consider that the light undergoes only one scattering event, *i.e.* we neglect multiple scattering paths, and that the nanostructures scatter light in a coherent manner. This is generally the case because the complete structure is typically a surface and only a few wavelengths large. Lastly, because we consider a one-dimensional (1D) ensemble of nanostructures, the scattered light remains in the plane of incidence, and we can model its direction with only one variable, the in-plane

wavevector (k_x).

Then, the far-field scattered amplitude by our nanostructures can be written as:

$$A(k_x) = \sum_n e^{ik_x x_n}, \quad (4)$$

and the scattered intensity is given by:

$$\begin{aligned} I(k_x) &= AA^* = \sum_n e^{ik_x x_n} \sum_m e^{-ik_x x_m} \\ &= \sum_n \sum_m e^{ik_x (x_n - x_m)}. \end{aligned} \quad (5)$$

Taking into account Eq. 1, this leads to the following expression for the ensemble averaged scattered intensity I (details in Supp Mat):

$$\begin{aligned} \langle I(k_x) \rangle &= N (1 - |\tilde{\rho}_\epsilon(k_x)|^2) \\ &+ |\tilde{\rho}_\epsilon(k_x)|^2 \left(\frac{\sin(\frac{Nk_x d}{2})}{\sin(\frac{k_x d}{2})} \right)^2 \\ &+ \sum_{m=1}^M [2(N - m) \cos(k_x m d) (\tilde{\rho}_{\Delta_m}(k_x) - |\tilde{\rho}_\epsilon(k_x)|^2)], \end{aligned} \quad (6)$$

where $\tilde{\rho}_\epsilon$ (resp. $\tilde{\rho}_\Delta$) is the Fourier Transform of the probability density function of ϵ (resp. Δ), and M is the number of nearby neighboring positions we consider correlated (equivalently, Md is the maximum distance at which we take into account correlations). Typically, $Md \geq 2L_c$ is sufficient with the disorder presented above.

In this formula, three terms can be identified, as highlighted by breaks in the typesetting. The first term corresponds to the diffuse background, typical of disordered structures, the second term is well known for Bragg peaks, as in, e.g., the grating formula, typical for periodic structures [23]. These terms are controlled by the PDF of ϵ , or more precisely by its Fourier Transform. This explains the progressive disappearance of the Bragg peaks when perturbations are added, starting from the higher order modes, as $\tilde{\rho}_\epsilon$ becomes a thinner Gaussian curve when $S_d = \text{Var}(\epsilon)$ increases.

The last term, however, has never been made explicitly apparent in the models describing scattering, and therefore its effect has been overlooked. It is the term which accounts for the influence of correlations, and is responsible for the correlation halos.

To better understand how each of these terms in Eq. 6 influences the scattered intensity distribution, Fig. 3 shows the shape of each term. The correlation term exhibits a slowly varying envelope due to the $\cos(k_x m d)$ term. It is the only term of the scattered intensity decomposition that can be negative, and thus make "holes" in the scattered background, which is non-decreasing as k_x moves away from the specular reflection. It is therefore paramount to understanding the absence of scattering around the specular reflection, typical of hyperuniform ensembles.

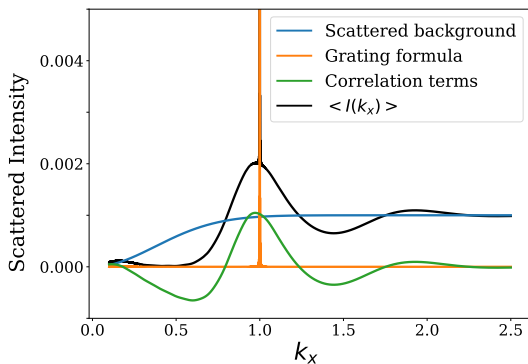


FIG. 3. Average scattered intensity of a correlated disordered structure generated with Eq. 2 ($S_d = 0.3$, $L_c = 1$), with the decomposition of the average intensity formula.

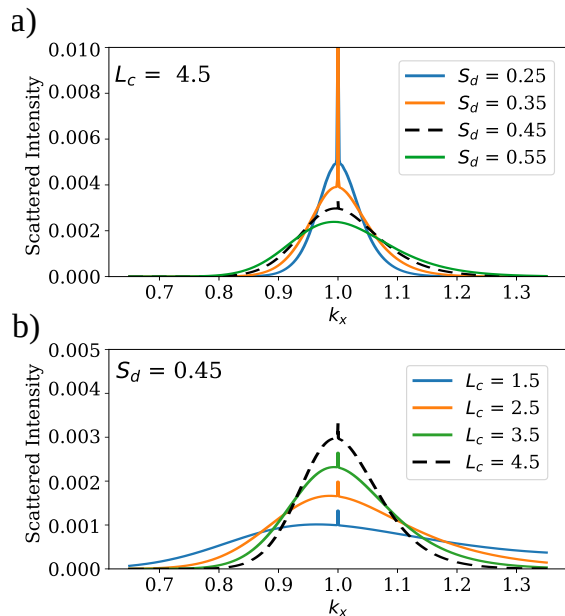


FIG. 4. Evolution of the average angular diagram of the scattered light around the first diffraction order as a function of a) S_d and b) L_c . The black dotted line is the one corresponding to Fig. 2.

Figure 4 shows a close-up of how the correlations halos are distributed around the first diffraction order and how they are influenced by S_d and L_c . Indeed, changing S_d influences mostly the diffraction peak height, but also the angular spread of the correlation halo (see Fig. 4a). A larger S_d leads to less diffraction, and for $S_d > 0.5$, no diffraction peak is visible. Changing L_c influences the correlation halo's angular size and maximum height, with no effect on the diffraction peak intensity (see Fig. 4b). This is expected, given that the diffraction peak intensity is only controlled by ρ_ϵ in Eq. 6, and therefore not sensitive to L_c . Interestingly, this means it is possible to independently design both the peak and halo sizes by choosing S_d and adjusting with L_c to achieve the desired scattering diagram.

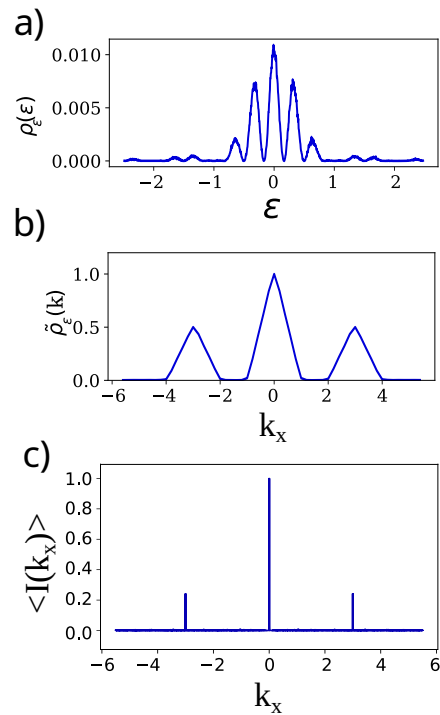


FIG. 5. Example of a probability distribution removing all diffracted orders except the third; a) $\rho_\epsilon(\epsilon)$ of an ensemble of nanostructures, b) Corresponding $|\tilde{\rho}_\epsilon(k)|$, c) Resulting scattered intensity. 1000 nanostructures, no averaging.

Until now, we have shown how different components of the angular distribution of the scattered intensity can be tuned with the S_d and L_c parameters. However, this concept can be taken further by directly engineering the probability density function of the disorder. This way, we are able to control both the diffuse background and the diffraction peaks. In other words, even without manipulating the correlation halo term (*i.e.*, without controlling L_c), to produce specific noises (*i.e.* ϵ functions), exotic scattered intensity distributions can be produced.

This is exemplarily shown in the probability density function, plotted in Fig. 5a), derived from:

$$\rho_\epsilon(\epsilon) = 2 \left(\frac{\sin(\pi\epsilon)}{\pi\epsilon} \right)^2 (\cos(2\pi q\epsilon) + 1). \quad (7)$$

The Fourier Transform of this function presents three triangular peaks (Fig. 5b) with $q = 3$). Indeed, the Fourier Transform of $(\sin(x)/x)^2$ is a triangular peak, and the \cos term creates duplicate peaks centered around $k_x = \pm q$. As a consequence, for $q = 3$, only diffraction orders at $k_x = 0, -3$ and $+3$ can be observed in the far field scattering pattern. Figure 5c) demonstrates that this is indeed the case.

It also shows that the intensity of the orders at -3 and $+3$ is 0.25, with the specular reflection intensity being 1. With this approach, it is impossible to reduce the energy in the specular reflection, as $\rho_\epsilon(\epsilon)$ must be positive. It is also impossible to design an asymmetric $I(k_x)$, as

$\rho_\epsilon(\epsilon)$ must be real. However, in practice, the form factor of the individual nanostructures could be leveraged for additional control[26, 27]. Intensity patterns for other q values are shown in the Supplementary Material.

All these properties generalize well to two dimensional (2D) structures, where the nanostructure positions are $\{(x, y)\}_n$. The derivation of the disorder generation and the scattered intensity formulas are found in the Supp. Mat.

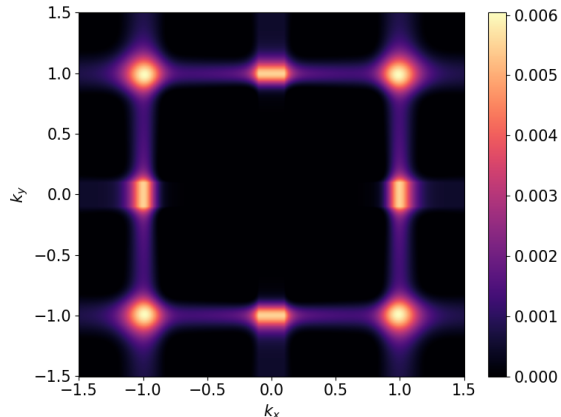


FIG. 6. Average scattered intensity for a 2D ensemble of 40x40 nanostructures. The disorder parameters are that of the 1D Morpho-like ensemble: $S_{d,x} = S_{d,y} = 0.4, L_{c,x} = L_{c,y} = 4.5$.

Figure 6 shows the resulting 2D scattered intensity distribution, along both k_x and k_y directions, showing 2D correlations halos centered on the Bragg Peak positions. The intensity values ($\sim 10^{-3}$) show that the scattered intensity distribution is smooth and not peaked, as Bragg peaks would have intensities close to 10^{-1} . By choosing different disorder variances S_d and correlation lengths L_c along x and y , asymmetric $I(k_x, k_y)$ can be obtained, mimicking scattering patterns observed in nature.

We have analytically modeled the angular distribution of scattered light reflected from a quasi-periodic assembly of nanostructures, by treating the perturbations added to the periodic positions as random variables whose properties can be controlled or measured. This novel approach has allowed us to explain the emergence of "correlation halos", broad scattering features that are neither Bragg peaks typical of periodic structures nor the diffuse background typical of uncorrelated disordered structures. The analytical model makes it possible to predict the shape of these halos, but also to design customized scattering diagrams. In addition, choosing the probability density functions for the perturbations applied to the periodic positions enables the design of structures with specific angular response. By defining design parameters that control the PDF, it is possible to use inverse design algorithms to generate multiple scattering diagrams and recover the underlying distributions, which is useful for future design of optical materials.

-
- [1] P. Vukusic, J. Sambles, C. Lawrence, and R. Wootton, Quantified interference and diffraction in single morpho butterfly scales, *Proceedings of the Royal Society of London. Series B: Biological Sciences* **266**, 1403 (1999).
 - [2] T. B. Schroeder, J. Houghtaling, B. D. Wilts, and M. Mayer, It's not a bug, it's a feature: functional materials in insects, *Advanced Materials* **30**, 1705322 (2018).
 - [3] S. R. Mouchet, S. Luke, L. T. McDonald, and P. Vukusic, Optical costs and benefits of disorder in biological photonic crystals, *Faraday Discussions* **223**, 9 (2020).
 - [4] B. D. Wilts, J. Otto, and D. G. Stavenga, Ultra-dense, curved, grating optics determines peacock spider coloration, *Nanoscale advances* **2**, 1122 (2020).
 - [5] E. Moyroud, T. Wenzel, R. Middleton, P. J. Rudall, H. Banks, A. Reed, G. Mellers, P. Killoran, M. M. Westwood, U. Steiner, *et al.*, Disorder in convergent floral nanostructures enhances signalling to bees, *Nature* **550**, 469 (2017).
 - [6] M. Rothhammer, C. Zollfrank, K. Busch, and G. von Freymann, Tailored disorder in photonics: learning from nature, *Advanced Optical Materials* **9**, 2100787 (2021).
 - [7] A. Saito, M. Yonezawa, J. Murase, S. Juodkazis, V. Mizeikis, M. Akai-Kasaya, and Y. Kuwahara, Numerical analysis on the optical role of nano-randomness on the morpho butterfly's scale, *Journal of Nanoscience and Nanotechnology* **11**, 2785 (2011).
 - [8] V. E. Johansen, Optical role of randomness for structured surfaces, *Applied Optics* **53**, 2405 (2014).
 - [9] B. Song, V. E. Johansen, O. Sigmund, and J. H. Shin, Reproducing the hierarchy of disorder for morpho-inspired, broad-angle color reflection, *Scientific reports* **7**, 46023 (2017).
 - [10] F. Sterl, E. Herkert, S. Both, T. Weiss, and H. Giessen, Shaping the color and angular appearance of plasmonic metasurfaces with tailored disorder, *ACS Nano* **15**, 10318 (2021).
 - [11] E. Herkert, F. Sterl, S. Both, S. G. Tikhodeev, T. Weiss, and H. Giessen, Influence of structural disorder on plasmonic metasurfaces and their colors—a coupled point dipole approach: tutorial, *JOSA B* **40**, B59 (2023).
 - [12] S. Torquato and F. H. Stillinger, Local density fluctuations, hyperuniformity, and order metrics, *Physical Review E* **68**, 041113 (2003).
 - [13] O. Leseur, R. Pierrat, and R. Carminati, High-density hyperuniform materials can be transparent, *Optica* **3**, 763 (2016).
 - [14] F. Bigourdan, R. Pierrat, and R. Carminati, Enhanced absorption of waves in stealth hyperuniform disordered media, *Optics Express* **27**, 8666 (2019).
 - [15] K. Vynck, R. Pierrat, R. Carminati, L. S. Froufe-Pérez, F. Scheffold, R. Sapienza, S. Vignolini, and J. J. Sáenz, Light in correlated disordered media, *Reviews of Modern Physics* **95**, 045003 (2023).
 - [16] M. A. Klatt, P. J. Steinhardt, and S. Torquato, Foam-

- tonic designs yield sizeable 3d photonic band gaps, *Proceedings of the National Academy of Sciences* **116**, 23480 (2019).
- [17] S. Yu, C.-W. Qiu, Y. Chong, S. Torquato, and N. Park, Engineered disorder in photonics, *Nature Reviews Materials* **6**, 226 (2021).
- [18] G. Jacucci, S. Vignolini, and L. Schertel, The limitations of extending nature’s color palette in correlated, disordered systems, *Proceedings of the National Academy of Sciences* **117**, 23345 (2020).
- [19] D. G. Stavenga, J. Tinbergen, H. L. Leertouwer, and B. D. Wilts, Kingfisher feathers – colouration by pigments, spongy nanostructures and thin films, *Journal of Experimental Biology* **214**, 3960 (2011).
- [20] K. Djeghdi, U. Steiner, and B. D. Wilts, 3d tomographic analysis of the order-disorder interplay in the pachyrhynchus congestus mirabilis weevil, *Advanced Science* **9**, 2202145 (2022).
- [21] H. Yin, B. Dong, X. Liu, T. Zhan, L. Shi, J. Zi, and E. Yablonovitch, Amorphous diamond-structured photonic crystal in the feather barbs of the scarlet macaw, *Proceedings of the National Academy of Sciences* **109**, 10798 (2012).
- [22] T. Welberry, Diffuse x-ray scattering and models of disorder, *Reports on Progress in Physics* **48**, 1543 (1985).
- [23] F. Leroy, R. Lazzari, and G. Renaud, Effects of near-neighbor correlations on the diffuse scattering from a one-dimensional paracrystal, *Acta Crystallographica Section A: Foundations of Crystallography* **60**, 565 (2004).
- [24] S. Yoshioka and S. Kinoshita, Wavelength-selective and anisotropic light-diffusing scale on the wing of the morpho butterfly, *Proceedings of the Royal Society B: Biological Sciences* **271**, 581 (2004).
- [25] M. A. Giraldo, S. Yoshioka, C. Liu, and D. G. Stavenga, Coloration mechanisms and phylogeny of morpho butterflies, *Journal of Experimental Biology* **219**, 3936 (2016).
- [26] B. Gralak, G. Tayeb, and S. Enoch, Morpho butterflies wings color modeled with lamellar grating theory, *Optics express* **9**, 567 (2001).
- [27] J. Boulenguez, S. Berthier, and F. Leroy, Multiple scaled disorder in the photonic structure of morpho rhetenor butterfly, *Applied Physics A* **106**, 1005 (2012).